



Development of carbohydrate-based nano-microstructures loaded with fish oil by using electrohydrodynamic processing

García Moreno, Pedro Jesús; Özdemir, N.; Boutrup Stephansen, Karen; Mateiu, Ramona Valentina; Echevoyend, Y. ; Lagaron, J.M. ; Chronakis, Ioannis S.; Jacobsen, Charlotte

Published in:
Food Hydrocolloids

Link to article, DOI:
[10.1016/j.foodhyd.2017.02.013](https://doi.org/10.1016/j.foodhyd.2017.02.013)

Publication date:
2017

Document Version
Peer reviewed version

[Link back to DTU Orbit](#)

Citation (APA):
García Moreno, P. J., Özdemir, N., Boutrup Stephansen, K., Mateiu, R. V., Echevoyend, Y., Lagaron, J. M., Chronakis, I. S., & Jacobsen, C. (2017). Development of carbohydrate-based nano-microstructures loaded with fish oil by using electrohydrodynamic processing. *Food Hydrocolloids*, 69, 273-285.
<https://doi.org/10.1016/j.foodhyd.2017.02.013>

General rights

Copyright and moral rights for the publications made accessible in the public portal are retained by the authors and/or other copyright owners and it is a condition of accessing publications that users recognise and abide by the legal requirements associated with these rights.

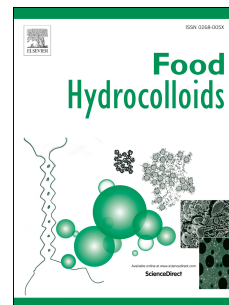
- Users may download and print one copy of any publication from the public portal for the purpose of private study or research.
- You may not further distribute the material or use it for any profit-making activity or commercial gain
- You may freely distribute the URL identifying the publication in the public portal

If you believe that this document breaches copyright please contact us providing details, and we will remove access to the work immediately and investigate your claim.

Accepted Manuscript

Development of carbohydrate-based nano-microstructures loaded with fish oil by using electrohydrodynamic processing

Pedro J. García-Moreno, Necla Özdemir, Karen Stephansen, Ramona V. Mateiu, Yolanda Echegoyen, Jose M. Lagaron, Ioannis S. Chronakis, Charlotte Jacobsen



PII: S0268-005X(16)30671-3

DOI: [10.1016/j.foodhyd.2017.02.013](https://doi.org/10.1016/j.foodhyd.2017.02.013)

Reference: FOOHYD 3802

To appear in: *Food Hydrocolloids*

Received Date: 26 October 2016

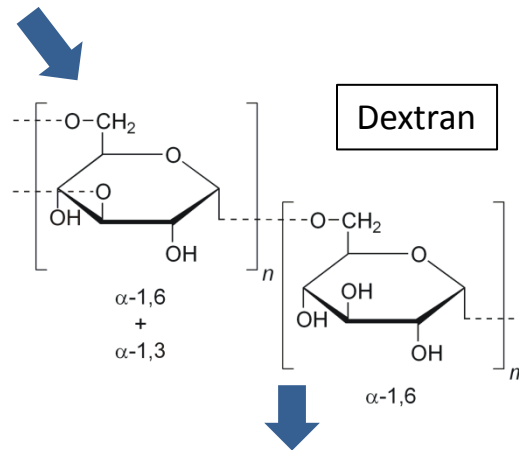
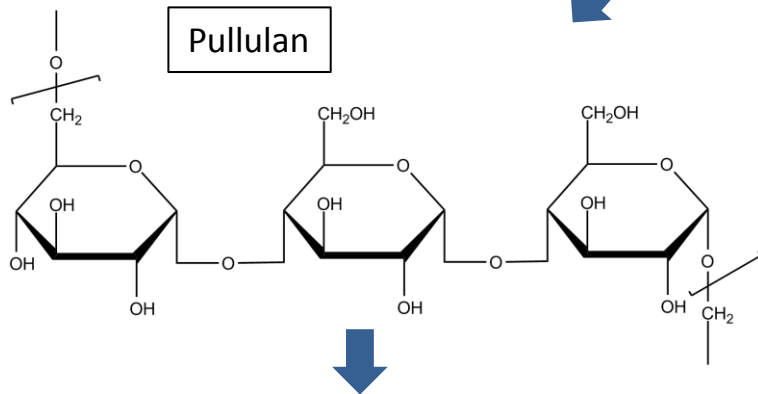
Revised Date: 27 January 2017

Accepted Date: 19 February 2017

Please cite this article as: García-Moreno, P.J., Özdemir, N., Stephansen, K., Mateiu, R.V., Echegoyen, Y., Lagaron, J.M., Chronakis, I.S., Jacobsen, C., Development of carbohydrate-based nano-microstructures loaded with fish oil by using electrohydrodynamic processing, *Food Hydrocolloids* (2017), doi: [10.1016/j.foodhyd.2017.02.013](https://doi.org/10.1016/j.foodhyd.2017.02.013).

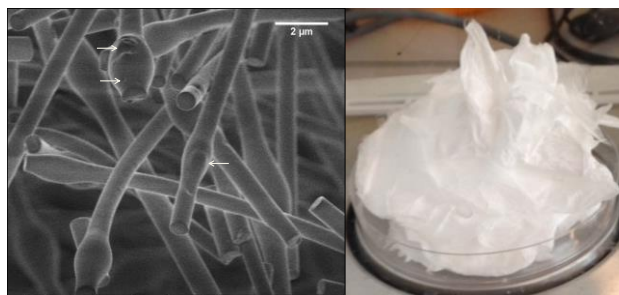
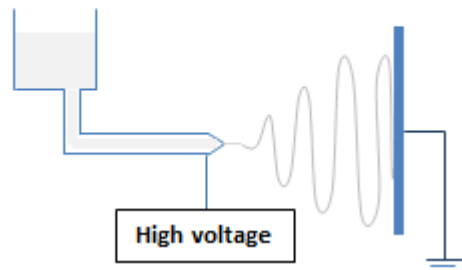
This is a PDF file of an unedited manuscript that has been accepted for publication. As a service to our customers we are providing this early version of the manuscript. The manuscript will undergo copyediting, typesetting, and review of the resulting proof before it is published in its final form. Please note that during the production process errors may be discovered which could affect the content, and all legal disclaimers that apply to the journal pertain.

Fish oil rich in omega-3 PUFA



Pullulan solution containing fish oil

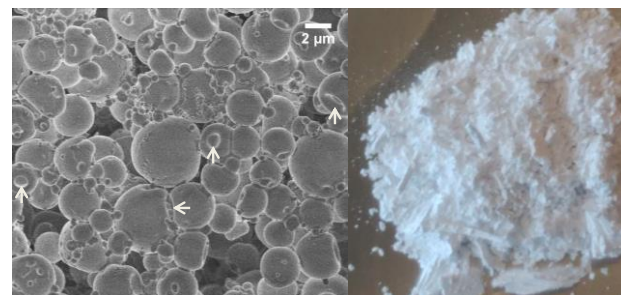
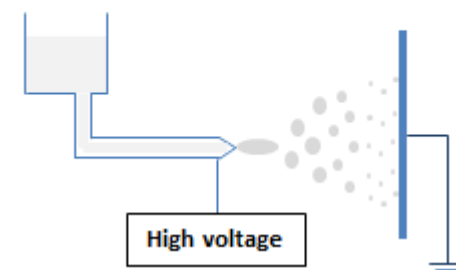
Electrospinning processing



Fish oil-loaded pullulan nanofibers

Dextran solution containing fish oil

Electrospraying processing



Fish oil-loaded dextran nanocapsules

1 **DEVELOPMENT OF CARBOHYDRATE-BASED NANO-**
2 **MICROSTRUCTURES LOADED WITH FISH OIL BY USING**
3 **ELECTROHYDRODYNAMIC PROCESSING**

4 Pedro J. García-Moreno^{a*}, Necla Özdemir^{a,b}, Karen Stephansen^a, Ramona V. Mateiu^c, Yolanda
5 Echegoyen^{d, †}, Jose M. Lagaron^d, Ioannis S. Chronakis^a, Charlotte Jacobsen^a

6 ^a Division of Food Technology, National Food Institute, Technical University of Denmark, Denmark

7 ^b Food Engineering Department, Ankara University, Turkey

8 ^c DTU CEN, Center for Electron Nanoscopy, Technical University of Denmark, Denmark

9 ^d Novel Materials and Nanotechnology Group, IATA-CSIC, Spain

10 [†] Present address: Science Education Department, Facultat de Magisteri, Universitat de València,
11 Spain

12 **ABSTRACT**

13 The encapsulation of fish oil in carbohydrate-based nanomicrostructures obtained by
14 electrohydrodynamic processing was investigated. Solutions of pullulan 200 kDa (15 wt.%) and
15 dextran 70 kDa (25 wt.%) presented appropriate properties (viscosity, surface tension and
16 conductivity) to allow the formation of nano-microfibers and nano-microcapsules, respectively.
17 Although dextran 70 kDa exhibited antioxidant properties in solution, their capsules produced at lab
18 and pilot-plant scales showed a low oxidative stability both with emulsified and neat oil. Phase
19 separation of solution and opened capsules indicated a poor interaction between dextran and fish oil,
20 which suggested that further optimization of the electro spraying solution is necessary. On the contrary,
21 pullulan solutions were optimized to work even at pilot-plant scale. In this case, in spite of the
22 prooxidant effect of pullulan in solution, oxidatively stable pullulan fibers (PV=12.3±0.9 meq O₂/kg
23 and 15.5±5.1 ng/g of 1-penten-3-ol) were obtained when oil was incorporated as neat oil and when
24 producing batches during short time (30 or 10 min). This superior oxidative stability when compared
25 to fibers with emulsified oil is mainly attributed to a higher fish oil entrapment and to the location of
26 the oil in large bead-structures with a reduced specific surface area. These results indicated the

* Corresponding author. Tel: +45 25 25 59; Fax: +45 45 88 47 74; E-mail: pejeg@food.dtu.dk

27 feasibility of producing omega-3 nanodelivery systems by encapsulating fish oil in pullulan nano-
28 microfibers using electrospinning processing.

29 **Keywords:** fish oil, pullulan, dextran, electrohydrodynamic processing, oxidative stability

30 1. INTRODUCTION

31 Long chain omega-3 polyunsaturated fatty acids (omega-3 PUFA), specially eicosapentaenoic
32 (C20:5n-3, EPA) and docosahexaenoic (C22:6n-3, DHA) acids, provide numerous beneficial effects
33 on human health such as prevention of cardiovascular diseases, improvement of anti-inflammatory and
34 allergic responses and development of brain and eye retina (Shahidi, 2015). As a consequence, the
35 demand of functional food and infant formulations enriched with these lipids, continues to increase in
36 North America and Europe, and it is expected to grow considerably in Asia through the next decade
37 (GOED, 2015). However, omega-3 PUFA are highly susceptible to oxidation and has a low solubility
38 in most food systems, which limit their use as nutritionally beneficial lipids in food (Encina, Vergara,
39 Giménez, Oyarzún-Ampuero, & Robert, 2016). To overcome these drawbacks, encapsulation of
40 omega-3 PUFA is commonly carried out, which makes it possible to mask their unpleasant taste and
41 odor and to protect these highly unsaturated fatty acids against prooxidants (e.g. oxygen, light, free
42 radicals and metal ions) (Comunian & Favaro-Trindade, 2016).

43 Electrohydrodynamic processing is an emerging encapsulation technique, which has been used to
44 obtain submicron encapsulates for both hydrophilic (bifidobacterium strain - López-Rubio, Sanchez,
45 Wilkanowicz, Sanz, & Lagaron, 2012; ferulic acid - Yang, Zha, Yu, & Liu, 2013; gallic acid- Neo,
46 Ray, & Jin, 2013 and (-)-epigallocatechin gallate - Gómez-Mascaraque, Sanchez, & López-Rubio,
47 2016) and hydrophobic (β -carotene - López-Rubio & Lagaron, 2012; curcumin - Brahatheeswaran et
48 al., 2012; and lycopene - Pérez-Masiá, Lagaron, & Lopez-Rubio, 2015) bioactive compounds. The
49 process employs a high-voltage electro-static field to charge the surface of a polymer solution droplet
50 at the end of a capillary tube. As a consequence of mutual charge repulsion, the droplet elongates
51 forming a conical shape known as the Taylor cone. When the electric field applied overcomes the
52 surface tension of the droplet, a charged jet of polymer solution is ejected from the tip of the Taylor

53 cone. If the jet is stable (e.g. due to high polymer chain entanglements), the process is called
54 electrospinning and micro- or nanofibers are produced after evaporation of the solvent during
55 elongation of the jet as a consequence of several instabilities (e.g. whipping or bending motions). On
56 the other hand, in the electrospraying process, due the low viscoelasticity of the polymer solution, the
57 jet subsequently breaks up and deposits on a grounded or oppositely charged collector as fine particles
58 (Ghorani & Tucker, 2015). Alternatively to the most common microencapsulation technique (spray-
59 drying), electrohydrodynamic processes (e.g. electrospinning or electrospraying) do not require the
60 use of a heated air stream, which avoids the deterioration of thermo- and oxygen-sensitive bioactive
61 compounds (Lim, 2015). Moreover, and contrarily to freeze-drying, electrohydrodynamic processes
62 can be up-scaled and run in continuous operation mode. In addition, nano-microstructures (NMS) (e.g.
63 fibers or capsules) obtained by electrohydrodynamic processing present a reduced size (0.1-5 μm),
64 which makes them easier to disperse in food matrices when compared to encapsulates produced by
65 traditional (e.g. spray- and freeze-drying, 1-100 μm) or other emerging encapsulation techniques (e.g.
66 co-acervation, 5-200 μm ; and extrusion, 15-2000 μm) (Barrow, Wang, Adhikari, & Liu, 2013).

67 Food-grade NMS are obtained by using biopolymers (e.g. proteins, polysaccharides), bio-compatible
68 polymers (e.g. poly-vinyl alcohol, PVA; polyethylene oxide, PEO) or their blends which are dissolved
69 in solvents approved for food applications (e.g. water, alcohols, formic and acetic acids) (Weiss,
70 Kanjanapongkul, Wongsasulak, & Yoovidhya, 2012). Common proteins used as encapsulating
71 materials are zein (Yang et al., 2013; Neo et al., 2013; Brahatheeswaran et al., 2012), whey protein
72 concentrate (WPC) (López-Rubio & Lagaron, 2012; Pérez-Masiá et al., 2015; Gómez-Mascarque,
73 Morfin, Pérez-Masiá, Sanchez, & Lopez-Rubio, 2016) and gelatin (Li, Zheng, & Han, 2006). Other
74 food-grade protein-based nano-microfibers have been obtained by using blends such as soy protein
75 isolate (SPI)-PVA (Cho, Netravali, & Joo, 2012), egg albumen-cellulose acetate (Wongsasulak,
76 Patapeejumruswong, Weiss, Supaphol, & Yoovidhya, 2010) and amaranth protein-pullulan (Aceituno-
77 Medina, Mendoza, Lagaron, & Lopez-Rubio, 2015). A great variety of polysaccharides, such as
78 pullulan (López-Rubio et al., 2012), dextran (Pérez-Masiá et al., 2015), chitosan (Gómez-Mascarque

79 et al., 2016a), starch (Pérez-Masiá, Lagaron, & Lopez-Rubio, 2014), chitosan-alginate blend
80 (Lertsutthiwong & Rojsitthisak, 2011) and alginate-pectin-PEO blend (Alborzi, Lim, & Kakuda,
81 2010), have also been employed as wall materials for the production of bioactive delivery-systems.
82 Nevertheless, to the best of the authors' knowledge, omega-3 PUFA encapsulates have only been
83 obtained by electrohydrodynamic processing when using PVA (García-Moreno et al., 2016) or
84 proteins such as zein (Torres-Giner, Martinez-Abad, Ocio, & Lagaron, 2010; Moomand & Lim., 2014)
85 and more recently SPI, gelatin and WPC (Gómez-Mascaraque & López-Rubio, 2016). In this regard, it
86 is worth noting that, contrarily to proteins, polysaccharides are suitable shell material under high
87 temperature processes due to their thermal stability (Fathi, Martín, & McClements, 2014). Thus, they
88 may increase the protection of omega-3 PUFA encapsulates when incorporated into food products
89 requiring heating for their production (e.g. baked products).

90 Therefore, this work aimed to study the development of carbohydrate-based encapsulates containing
91 omega-3 PUFA by electrohydrodynamic processes. Particularly, two neutral polysaccharides of
92 microbial origin, namely pullulan and dextran, were evaluated as encapsulating materials. Pullulan is a
93 linear glucan consisting of maltotriose units connected by α -1,6 glycosidic bonds; whereas dextran has
94 a branched structure with α -1,6-glucose-linkages with side-chains attached to the 3-positions of the
95 backbone glucose units. Both polysaccharides are water soluble, biocompatible and biodegradable,
96 and are used in food and pharmaceutical applications (Park & Khan, 2009). First, the influence of
97 polysaccharide concentration on the physical properties (e.g. viscosity, conductivity and surface
98 tension) of the solutions and on the morphology of NMS loaded with fish oil was assayed. Secondly,
99 the oxidative stability during storage of polysaccharide solutions containing fish oil was determined.

100 Finally, selected NMS (e.g. pullulan nano-microfibers and dextran nano-microcapsules) were
101 produced, both in lab and pilot-plant scale, by incorporating the fish oil as emulsified or as neat oil.
102 The effect of the oil-incorporation approach on the morphology, lipid distribution and oxidative
103 stability of the NMS was investigated.

104 2. MATERIALS AND METHODS

105 2.1 Materials

106 Pullulan (molecular weight = 200,000 Da) was kindly donated by Hayashibara Co., Ltd. (Okayama,
107 Japan). Dextran (molecular weight = 70,000 Da, dextran70) was generously provided by
108 Pharmacosmos A/S (Holbaek, Denmark). Dextran (molecular weight = 500,000 Da, dextran500) was
109 kindly supplied by Dextran Products Limited (Ontario, Canada). Whey protein concentrate (WPC),
110 under the commercial name of Lacprodan® DI-8090, was kindly donated by ARLA Food Ingredients
111 (Viby, Denmark). Commercial cod liver oil was kindly provided by Maritex A/S, subsidiary of TINE,
112 BA (Sortland, Norway) and stored at -40 °C until use. The fatty acid composition of the fish oil was
113 determined by fatty acid methylation (AOCS, 1998a) followed by separation through GC (AOCS,
114 1998b). It was (major fatty acids only) as follows: C16:0, 9.5%; C16:1, 8.7%; C18:1, 16.3%; C20:1,
115 12.6%; C20:5, 9.2% and C22:6, 11.4%. The tocopherol content of the fish oil was: α -tocopherol,
116 200 ± 3 $\mu\text{g/g}$ oil; β -tocopherol, 5 ± 1 $\mu\text{g/g}$ oil; γ -tocopherol, 96 ± 3 $\mu\text{g/g}$ oil and δ -tocopherol, 47 ± 1 $\mu\text{g/g}$
117 oil (AOCS, 1998c). The peroxide value (PV) of the fish oil used was 0.38 ± 0.04 meq/kg oil. Whey
118 protein isolate (WPI), with commercial name Laprodan® DI-9224, was kindly donated by ARLA
119 Food Ingredients. All other chemicals and solvents used were of analytical grade.

120 2.2 Preparation of biopolymer solutions containing fish oil

121 For the evaluation of the influence of biopolymer type and concentration on solution properties and
122 NMS morphology, polysaccharides were assayed at the following concentrations: pullulan, 5-10-15
123 wt.%; dextran70, 20-30-40 wt.%; and dextran500, 10-20-30 wt.%. NMS morphology was also studied
124 when using a solution of dextran70 at 25 wt.%. The selected ranges of concentration aimed to obtain
125 different nano-microstructures morphology (e.g. fibers or capsules), and they are based on the type
126 and molecular weight of the biopolymers. WPC, which has been widely used for the encapsulation of
127 bioactives, was also tested as a control at 10-20-30 wt.%. Biopolymers were dissolved in distilled
128 water under constant stirring at room temperature. Fish oil, accounting for 10 wt.% with respect to
129 biopolymer, was added as 10 wt.% fish oil-in-water emulsion stabilized with 1 wt.% WPI at pH 7. The

130 homogenization process was carried out by using a microfluidizer (M110L Microfluidics, Newton,
131 MA, USA) as described elsewhere (García-Moreno, Guadix, Guadix, & Jacobsen, 2016), resulting in
132 an emulsion with $D_{3,2}=134\pm 1$ nm. The biopolymer solutions and the fish oil-in-water emulsion were
133 mixed under nitrogen atmosphere by using magnetic stirring for 30 min at 5 °C in the dark. Samples
134 were used immediately after production for electrospinning processing and subsequently stored at 5 °C
135 in the dark until analysis of solution properties.

136 Selected solutions, namely 15 wt.% pullulan and 25 wt.% of dextran70, were prepared for studying the
137 oxidative stability of NMS. Fish oil was incorporated both as emulsion (as previously described) and
138 as neat oil by using 20 wt.% Tween-20 (with respect to fish oil) as emulsifier. Tween-20 was added to
139 the biopolymer solution and mixed using mechanical stirring for 10 min at 500 rpm under nitrogen
140 atmosphere. Subsequently, neat fish oil, accounting for the 10 wt.% of the biopolymer, was dispersed
141 in the previous solution using mechanical stirring for 20 min at 500 rpm under nitrogen atmosphere.
142 Samples were used immediately after production for electrospinning and electrospaying.

143 **2.3 Characterization of solutions**

144 The different biopolymer solutions containing emulsified fish oil were characterized in terms of
145 viscosity, conductivity, surface tension, droplet size distribution and oxidative stability.

146 **2.3.1 Viscosity, surface tension and conductivity**

147 Viscosity was measured using a stress controlled rheometer Stresstech (Reologica Instruments AB,
148 Lund, Sweden) equipped with a CC25 standard bob cup system in a temperature vessel at 25°C.
149 Surface tension was measured using the Wilhelmy plate method at room temperature in a K10ST
150 tensiometer (Krüss GmbH, Hamburg, Germany). Electrical conductivity was determined in a
151 conductivity meter LF 323 (WTW GmbH, Weilheim, Germany) at 25°C. All determinations were
152 performed in triplicate.

153 **2.3.2 Droplet size distribution**

154 Droplet sizes were measured by laser diffraction in a Mastersizer 2000 (Malvern Instruments, Ltd.,
155 Worcestershire, UK). Solutions were diluted in recirculating water (3000 rpm), until it reached an

156 obscuration of 12%. The refractive indices of sunflower oil (1.469) and water (1.330) were used as
157 particle and dispersant, respectively. Measurements were made in triplicate after production.

158 **2.3.3 Oxidative stability**

159 For lipid oxidation measurements, immediately after production, biopolymers solutions (15 wt.%
160 pullulan, 30 wt.% dextran70, 20 wt.% dextran500 and 30 wt.% WPC) containing emulsified fish oil
161 were stored in 100 mL brown bottles at 40 °C in the dark for 14 days. Each bottle contained 40 g of
162 solution. Emulsified fish oil (10 wt.% fish oil-in-water emulsion; stabilized with 1 wt.% WPI) was
163 also analyzed. Samples were taken at day 0, 4, 9 and 14 for analysis.

164 *2.3.3.1 Determination of peroxide value and tocopherol content*

165 Lipids were extracted from solutions according to Bligh and Dyer method using a reduced amount of
166 the chloroform/methanol (1:1, wt.%) solvent (Bligh & Dyer, 1959). Two extractions were made from
167 each sample. Peroxide value was determined on lipid extracts using the colorimetric ferric-thiocyanate
168 method at 500 nm as described by Shantha and Decker (1994). For tocopherol determination, lipid
169 extracts (1–2 g) were weighed off and evaporated under nitrogen and re-dissolved in heptane prior to
170 analysis according to AOCS (1998).

171 *2.3.3.2 Secondary oxidation products – Dynamic headspace GC-MS*

172 Approximately 4 g of solutions and 30 mg internal standard (4-methyl-1-pentanol, 30 µg/g water)
173 were weighted out in a 100 mL purge bottle, to which 5 mL of distilled water and 1 mL antifoam
174 (Synperonic 800 µL/L water) were added. The bottle was heated to 45°C in a water bath while purging
175 with nitrogen (flow 150 mL/min, 30 min). Volatile secondary oxidation products were trapped on
176 Tenax GR tubes. The volatiles were desorbed again by heating (200°C) in an Automatic Thermal
177 Desorber (ATD-400, Perkin Elmer, Norwalk, CN), cryofocused on a cold trap (-30°C), released again
178 (220°C), and led to a gas chromatograph (HP 5890IIA, Hewlett Packard, Palo Alto, CA, USA;
179 Column: DB-1701, 30 m x 0.25 mm x 1.0 µm; J&W Scientific, CA, USA). The oven program had an
180 initial temperature of 45°C for 5 min, increasing with 1.5°C/min until 55°C, with 2.5°C/min until

181 90°C, and with 12.0°C/min until 220°C, where the temperature was kept for 4 min. The individual
182 compounds were analyzed by mass-spectrometry (HP 5972 mass-selective detector, Agilent
183 Technologies, USA; electron ionization mode, 70 eV; mass to charge ratio scan between 30 and 250).
184 Emulsified fish oil (10 wt.% oil-in-water emulsion, stabilized with 1 wt.% WPI) was also analyzed
185 following the same procedure. The individual compounds were identified by both MS-library searches
186 (Wiley 138 K, John Wiley and Sons, Hewlett-Packard) and by authentic external standard and
187 quantified through calibration curves. The external standards employed were 2-ethylfuran, 1-penten-3-
188 one, 1-penten-3-ol, (*E*)-2-pentenal, hexanal, (*E*)-2-hexenal, (*E,E*)-2,4-heptadienal, (*E,Z*)-2,6-
189 nonadienal and (*E*)-2-decenal (Sigma-Aldrich, Brøndby, Denmark).

190 **2.4 Electrohydrodynamic process**

191 In lab scale, the electrohydrodynamic process was carried out by adding the biopolymer solutions
192 containing the fish oil to a syringe which was placed in a syringe pump (New Era Pump Systems, Inc.,
193 USA). The syringe pump delivered solutions with a flow rate of 0.01 ml/min. A 16 G needle (Proto
194 Advantage, Canada) was used. Using a high voltage power supply (Gamma High Voltage Research,
195 USA), an electric field of 20 kV was applied between the spinneret of the syringe and a 15 × 15 cm
196 collector plate made of stainless steel with alumina foil wrapped around it. The distance between the
197 syringe tip and the collector plate was 15 cm. The electrospinning process was conducted at room
198 temperature. NMS were produced in batches during 30 and 120 min under nitrogen atmosphere. A
199 schematic diagram of the lab facilities used for electrospinning and electrospraying processes is shown
200 in the Supplementary Material (Fig. S1).

201 Selected solutions were tested for production of NMS in pilot-plant scale. For that purpose, Fluidnatek
202 LE-100 (Bioinicia and Fluidnatedk®, Valencia, Spain) was employed. NMS were produced at room
203 temperature in batches during 10 min by using 24 needles with an inner diameter of 0.6 mm. Pullulan
204 solutions were processed at a flow rate of 5 mL/h by applying an electric field of 35 kV between the
205 needles and the collector, which were placed at 15 cm distance. In the case of dextran solutions, an
206 electric field of 42 kV was applied and the distance used between the needles and the collector was 10

207 cm. Different processing conditions were used in lab and pilot-plant scales since the pilot-plant scale
208 equipment allowed to apply a higher voltage when compared to the voltage source used in lab scale.
209 This allowed to obtain a stable Taylor cone (at least for pullulan solutions) at higher flowrates when
210 using the pilot-plant equipment, which is desirable to increase the productivity of the process.

211 **2.5 Characterization of NMS**

212 **2.5.1 Morphology**

213 The morphology of the NMS for the different biopolymers concentrations was investigated using
214 scanning electron microscopy (SEM) (FEI Inspect, Hillsboro, OR, USA). Approximately 0.5×0.5 cm
215 of the NMS sheet was placed on carbon tape and sputter coated with gold, 10 s, 40 mA utilizing a
216 Cressington 208HR Sputter Coater (Cressington Scientific Instruments, Watford, England).

217 Selected NMS were cut under liquid nitrogen and imaged in an FEI Helios dual beam scanning
218 electron microscope in high vacuum at room temperature by monitoring the secondary electrons with
219 the Through-The-Lens detector. No sample coating was used, instead the charge balance approach was
220 used. The fiber diameter and the bead size were determined from the micrographs by using the open
221 source image processing program ImageJ (National Institutes of Health). One hundred random fibers
222 were measured at 10 different points and all the beads, if presented. The number beads/area was
223 measured on all the micrographs presenting beads.

224 **2.5.2 Lipid encapsulation and distribution**

225 Fourier transform infrared (FT-IR) analysis was carried out in order to detect the presence of fish oil in
226 selected NMS. Transmission FT-IR experiments of control NMS (containing biopolymer and
227 Tween20) and NMS with emulsified and neat oil were recorded in a controlled chamber at 21°C with a
228 FT-IR Tensor 37 equipment (Bruker, Germany). Samples of 2 mg of NMS were gently mixed and
229 dispersed in 120 mg of spectroscopic grade KBr. The KBr pellets were prepared by first milling the
230 KBr and then adding the encapsulated powder into the milled KBr with gentle mixing. It allowed to
231 retain the existing composition of the encapsulates when entrapped in the pellet. Attenuated total
232 reflection mode (ATR) was only used for the analysis of fish oil and pure electrospun polymers

233 coupling the ATR accessory GoldenGate of Specac Ltd. (Orpington, UK) to the above-mentioned FT-
234 IR equipment. All spectra were recorded within the wavenumber range of 4000-600 cm^{-1} by averaging
235 20 scans at 4 cm^{-1} resolution.

236 Encapsulation efficiency (EE) of selected NMS was determined by measuring the non-entrapped fish
237 oil according to Moomand and Lim (2014) with some modifications. NMS (50 mg) were submerged
238 in heptane (10 mL) and gently shaken (100 rpm) for 15 min. The mixture was filtered and the
239 absorbance of the liquid was measured at 250 nm (UV-1800, Shimadzu, Japan). The amount of oil
240 present in the liquid was determined from a calibration curve ($R^2=0.99$), prepared by dissolving
241 various quantities of fish oil in heptane. The EE was calculated as:

$$242 \quad EE (\%) = \frac{A-B}{A} * 100 \quad [1]$$

243 where A is the total theoretical amount of fish oil and B is the free amount of fish oil in the collection
244 solution. Measurements were carried out in triplicate.

245 The lipid distribution of selected NMS was investigated by cutting them under liquid nitrogen and
246 imaging their cross-sections with the FEI Helios dual beam scanning electron microscope, as
247 described above. Furthermore, wet-scanning transmission electron microscopy in environmental SEM
248 mode was also carried out using a FEI Quanta 200F FEG for selected NMS in order to determine the
249 lipid distribution in the ultrathin fibers.

250 **2.5.3 Oxidative stability**

251 After production, analyses of PV and secondary oxidation products of selected NMS were carried out.
252 Lipids were extracted from NMS according to Bligh and Dyer method and PV determined as
253 previously described. Secondary oxidation products were also measured as described above, using 100
254 mg of NMS in each bottle, which was purged with nitrogen (flow 240 mL/min, 30 min). The external
255 standards employed were 2-ethylfuran, 1-penten-3-one, 1-penten-3-ol, (*E*)-2-pentenal, hexanal, (*E*)-2
256 hexenal, (*E,E*)-2,4-heptadienal, octanal and nonanal (Sigma-Aldrich, Brøndby, Denmark).

257 **2.6 Statistical analysis**

258 Statgraphics Centurion XV (Statistical Graphics Corp., Rockville, MD, USA) was used for data
259 analysis. Data were expressed as mean \pm standard deviation. Firstly, multiple sample comparison
260 analysis was performed to identify significant differences between samples. Secondly, mean values
261 were compared by using the Tukey's test. Differences between means were considered significant at p
262 < 0.05 .

263 **3. RESULTS AND DISCUSSION**

264 **3.1 Solutions properties and morphology of NMS**

265 Solution properties such as viscosity, surface tension and conductivity, which are critical for the
266 success of electrohydrodynamic processing, are shown in Table 1. These physical properties, which
267 are mainly dependent on the type of solvent, polymer molecular weight and concentration, affected the
268 morphology of the nano-microstructures obtained (Fig. 1). A particularly important parameter is
269 viscosity, which can be used as an indication of the degree of polymer chain entanglements in the
270 solution (Weiss et al., 2012). As expected, viscosity increased with increasing biopolymer
271 concentration for all solutions; for pullulan, dextran70, and dextran500 a considerable increase in
272 viscosity was observed when increasing the concentration from 5, 20 and 10 wt.% to 15, 40 and 30
273 wt.%, respectively (Table 1). It should be noted that dextran500 solutions showed a considerably
274 higher viscosity when compared to dextran70 solutions at the same concentration, which is explained
275 by the higher molecular weight of dextran500. Looking at the morphology of the corresponding NMS,
276 it is evident that the increase in viscosity was associated with formation of fibers instead of capsules
277 (Fig. 1C, 1F, 1I). This is in line with the results found by Stijnman, Bodnar, & Hans Tromp. (2011)
278 who reported fiber formation from 15 wt.% aqueous solutions of pullulan 200 kDa. Similar to our
279 results, Ritcharoen et al. (2008) also reported the production of fibers from 40-55 wt.% aqueous
280 solutions of dextran 70 kDa. It is worth mentioning that for dextran70 (40 wt.%) and dextran500 (30
281 wt.%), the fibers contained large amounts of beads (Fig. 1F, I). The presence of beads was not due to
282 the surface tension of these solutions when compared to pullulan solution (15 wt.%) (Table 1).

283 Dextran500 and specially dextran70 solutions had lower surface tension than pullulan solutions, which
284 should have allowed the electric forces to overcome the surface tension to initiate the jet more easily
285 resulting in the formation of fiber with less beads defects (Chronakis, 2010). This was not observed,
286 suggesting that the formation of beaded fibers for dextran70 and dextran500 might be related to
287 differences in chain entanglements exhibited by these polymers when compared to pullulan (even at
288 similar values of viscosity). The decrease in surface tension for dextran70 solutions when increasing
289 concentration was remarkable, indicating emulsifying properties for this polymer. In terms of
290 conductivity, dextran500 solutions showed considerably higher values when compared to pullulan and
291 dextran70 (Table 1). This might be most likely to their different ash content: 1.0 wt.% for dextran500
292 and no more than 0.1 wt.% for dextran70 and pullulan (data on ash content were provided by the
293 suppliers). Conductive polymer solutions will favor the production of more uniform fibers due to an
294 increase of mutual charge repulsion within the jet leading to a further elongation of the jet
295 (Ramakrishna, 2005). However, in highly conductive solutions, such as dextran500 solutions, the
296 effective repulsion force for stretching the fiber is reduced due to sliding of excess charge along the
297 surface of the polymer jet; this can lead to irregular electrospun materials (Lim, 2015).

298 WPC exhibited poor NMS-forming properties, requiring high polymer concentration in order to have
299 sufficient chain entanglement (Table 1). Even though it was possible to form capsules from WPC (Fig.
300 1K, L), a large amount of irregular morphologies was observed during production of the particles. The
301 irregular morphologies may be overcome by adding a surfactant (e.g. Tween-20) to the
302 electrospinning solution, which reduces the surface tension of the WPC-water solution, thus
303 improving the sprayability (Pérez-Masiá et al., 2015; Gómez-Mascaraque et al., 2016b). Contrarily,
304 dextran, both 70 and 500 kDa, led to the formation of spherical capsules at 20 wt.% concentration of
305 polymer (Fig. 1D, H). Similarly, capsules of dextran 70 kDa containing lycopene were also reported
306 by Pérez-Masiá et al. (2015). Solution of 25 wt.% dextran70 also led to capsules, allowing an increase
307 in the production rate of NMS when compared to the 20 wt.% dextran70 solution. For dextran500,
308 capsules with fibril defects were observed at 20 wt.% due to its higher molecular weight which
309 favored more polymer chain interactions (Fig. 1H).

310 **3.2 Droplet size distribution and oxidative stability of solutions**

311 The distribution of the lipids in the biopolymer solutions has a great influence on the lipid entrapment
312 and distribution in the final NMS (García-Moreno et al., 2016). Moreover, it may affect the oxidative
313 stability of the solutions during storage due to differences in the surface area. Therefore, the effect of
314 blending the emulsified oil with the biopolymer solutions on the droplet size distribution was
315 evaluated. It was observed that the addition of pullulan and dextran70 did not modify the droplet size
316 distribution of the parent emulsion ($D_{3,2}=134\pm 1$ nm). On the other hand, dextran500 and WPC
317 solutions had significantly larger droplets when compared to the parent emulsion; with $D_{3,2}=270\pm 1$ nm
318 and $D_{3,2}=207\pm 5$ nm, respectively (see Fig. S2 of the Supplementary Material). This could be attributed
319 to the presence of non-adsorbed biopolymers in the continuous phase which are capable of promoting
320 droplet flocculation through a depletion mechanism. Unadsorbed biopolymers can promote association
321 of oil droplets by inducing an osmotic pressure gradient within the continuous phase surrounding the
322 droplets (Singh & Ye, 2009). For each biopolymer, this phenomenon occurs above a critical
323 flocculation concentration, which is dependent on the effective volume of the biopolymer in aqueous
324 solution (Chanamai & McClements, 2001). This explains the differences observed between dextran70
325 and dextran500, having the latter a higher effective volume.

326 The oxidative stability of biopolymer solutions containing emulsified fish oil was investigated in order
327 to determine the effect of each biopolymer on fish oil oxidation (e.g. anti- or prooxidant). Fig. 2 shows
328 the content of primary oxidation products (e.g. hydroperoxides) in biopolymer solutions during
329 storage. A lag phase of four days was observed for the emulsion without any biopolymer (control),
330 followed by a significant increase in PV during the rest of the storage period (up to 7.6 ± 0.1 meqO₂/kg
331 oil at day 14). Dextran70 and WPC exhibited an antioxidant effect ($PV < 5$ meqO₂/kg oil), with
332 dextran70 solution resulting in a longer lag phase (9 days) and WPC solution maintaining the initial
333 low PV. On the contrary, pullulan and dextran500 solutions did not show any lag phase and both
334 polysaccharides thus exhibited a prooxidant effect on lipid oxidation (Fig. 2). These results correlated
335 well with the α -tocopherol content of the solutions after storage. Thus, dextran70 and WPC solutions
336 had a lower consumption of this endogenous antioxidant when compared to pullulan and dextran500

337 (see Fig. S3 of the Supplementary Material). Likewise, pullulan solutions had the highest content of
338 secondary oxidation products (Fig. 3a-d), followed by dextran500 solutions when considering 2-
339 ethylfuran and (*E,E*)-2,4-heptadienal volatiles (Fig. 3a, d). Dextran70 and WPC solutions had a lower
340 content of volatiles than pullulan and dextran500 solutions, apart from 1-penten-3-ol and (*E*)-2-
341 hexenal where dextran70 and WPC solutions were the second most oxidized, respectively (Fig. 3).

342 The low lipid oxidation observed for solutions containing WPC is explained by the recognized
343 antioxidant properties of whey protein such as chelation of transition metals by lactoferrin and free
344 radicals scavenging by amino acids containing sulfhydryl groups (e.g. cysteine) (Tong, Sasaki,
345 McClements, & Decker, 2000). The protection effect of dextran70, which was not observed for
346 dextran500, may be related to the differences observed in the droplet size distribution of the solutions.
347 Dextran500 solution showed flocculation and/or coalescence, which may change the interface and
348 thereby making the oil more accessible to prooxidants. Moreover, the surface activity of dextran70
349 (Table 1), may allow the incorporation of this polysaccharide (which is in excess in the solution) to the
350 interface of the oil droplets, increasing the protection of the lipids. Similarly, this mechanism was also
351 proposed by Matsumura et al. (2003) in order to explain the antioxidant effect of gum arabic and a
352 soluble soybean polysaccharide in oil-in-water emulsions stabilized with β -casein. These authors also
353 found a prooxidant behavior of pullulan in oil-in-water emulsions, both on the formation of
354 hydroperoxides and secondary oxidation products (e.g. malondialdehyde). Contrary to other complex
355 polysaccharides having protein moieties (e.g. gum arabic), pullulan did not show free radical
356 scavenging activity (Matsumara et al., 2003). Moreover, it did not present surface activity (Table 1),
357 which could have led to an interface with improved properties. The absence of these properties,
358 together with the fact that pullulan had a higher content of metals (130 ppm), which catalyze lipid
359 oxidation, when compared to WPC and dextran70 (< 2 ppm) might be the reason for the lower
360 oxidative stability of pullulan solutions (data on heavy metals content were provided by the suppliers).

361 **3.3. Characterization of selected NMS: emulsified vs. neat oil**

362 As a consequence of the satisfactory results obtained on the morphology of the NMS and on the
363 droplet size distribution of the biopolymers solutions, 15 wt.% pullulan and 25 wt.% dextran70
364 solutions were chosen for fiber- and particle-based lipid encapsulation, respectively. Moreover, the
365 protective effect of dextran70 against lipid oxidation in solution supported this selection. Although
366 pullulan exhibited a prooxidant effect in solution, it may protect the oil when obtaining dried
367 encapsulates (e.g. fibers) due to its inherent properties as a barrier for oxygen (Bakry et al., 2016).
368 Nonetheless, it is worth mentioning that, due to the high solubility of pullulan in water which
369 negatively affects to its oxygen barrier properties, pullulan fibers containing fish oil should only be
370 considered to be used as omega-3 delivery systems in dry food products. Contrary to the properties of
371 electrosprayed nano-microcapsules, the dimensional and morphological nature of electrospun nano-
372 microfibers (e.g. continuous in length) has limited their application in food, except for their use in
373 bioactive packaging strategies (Lopes da Silva, 2012). Therefore, further research is needed to explore
374 the encapsulating potential of electrospun fibers in food and one interesting possibility could be their
375 incorporation into multi-layered food systems. For instance, fish oil-loaded pullulan fibers may be
376 successfully incorporated in multi-layered granola bars, but this requires further evaluation.

377 **3.3.1. Morphology**

378 The three types of pullulan nano-microfibers produced at lab scale present circular cross-sections,
379 which were filled up either with pullulan and/or fish oil (Fig. 4-c). Nevertheless, differences in
380 morphology were observed for pullulan fibers containing emulsified oil compared to fibers with neat
381 oil and control pullulan fibers (with no added oil). Fibers containing neat oil presented the largest
382 diameter (75 % of fibers with diameter between 800 and 1100 nm), followed by fibers with emulsified
383 oil (83 % of fibers with diameter between 600 and 800 nm) and control fibers (80 % of fibers with
384 diameter between 500 and 700 nm) (Fig. 4d). The larger diameter of the fibers containing fish oil
385 compared to the control ones can be explained by an increase in solution viscosity due to the addition
386 of fish oil; from 878.0 ± 0.4 cP for the control solution to 1010.0 ± 16.0 and 1040.0 ± 26.0 cP for the
387 solutions containing neat and emulsified oil, respectively. Similarly, García-Moreno et al. (2016) and

388 Moomand and Lim (2015) reported an increase in fiber diameter when augmenting fish oil load in
389 PVA and zein fibers, respectively. Nevertheless, these authors obtained fibers with smaller diameters;
390 95% of PVA fibers were between 100-150 nm and 90 % of zein fibers were between 100-400 nm. For
391 fibers containing neat oil, the supplementary addition of Tween20, which led to an increase in the lipid
392 content (up to 12 wt.%), might be responsible for the larger diameter of this type of fibers when
393 compared to fibers containing emulsified oil. Moreover, fibers with neat oil exhibited the poorest
394 thickness uniformity since they had the broadest diameter distribution (Fig. 4d) and the largest
395 standard deviation from the fiber average diameter (Fig. 4e). In addition, fibers with emulsified oil
396 presented approximately 14 times less bead-defects than fibers with neat oil (47 beads/14,612 μm^2
397 versus 100 beads/2,281 μm^2). It has to be mentioned that these are relative numbers as they represent
398 the visualized areas which are prone to have artefacts caused by sample inhomogeneity and/or sample
399 preparation (e.g. transfer and cutting). In any case, the size of the beads for fibers with neat oil were
400 considerably larger (Fig. 4f). This cannot be attributed to differences in viscosity, since both solutions
401 (with emulsified and neat oil) contained the same concentration of pullulan and fish oil which are the
402 main factors determining viscosity. It can neither be explained by a superior surface tension value of
403 the solution with neat oil, since that solution contained Tween20 which favors jetting and avoids the
404 formation of beads (Pérez-Masiá, Lagaron, & Lopez-Rubio, 2014). However, these differences in
405 morphology may be attributable to a different distribution of fish oil in the two solutions. Emulsified
406 oil was homogenized in a high-pressure homogenizer before mixing with pullulan, leading to a very
407 fine emulsion ($D[0.5]=162\pm 1$ nm). On the other hand, neat oil was added to the pullulan solution
408 containing Tween20 and mixed mechanically, which led to a final coarse emulsion ($D[0.5]=2748\pm 1$
409 nm). As a consequence, the large droplets presented in the neat oil solution could not be incorporated
410 inside the fibers resulting in large bead structures. Similar observations were reported by García-
411 Moreno et al. (2016) and Arcchi, Mannino, & Weiss (2010) in PVA fibers when increasing the load
412 of emulsified fish oil and emulsified hexadecane, respectively. Likewise, production of pullulan fibers
413 with emulsified or neat oil at pilot-plant scale led to the same differences in morphology, although the
414 diameter of both types of fiber was smaller when compared to fibers obtained at lab scale (see Fig. S4

415 of the Supplementary Material). Although the higher flowrate employed in pilot-plant scale could
416 have favored an increase in fiber diameter, the superior voltage used causes greater stretching of the
417 solution by increasing the electrostatic repulsive force which ultimately led to a reduction in the fiber
418 diameter (Bhardwaj & Kundu, 2010).

419 Fig. 5 shows the morphology of the three types of dextran capsules produced at lab scale; without oil
420 (Fig. 5a), with emulsified (Fig. 5b) and neat oil (Fig. 5c). In general, the particles obtained were
421 almost spheres with an opened part such as a toroid shape (marked by arrows in Fig. 5). They also
422 presented a broad size distribution including both small (<300 nm) and large (>1000 nm) capsules.
423 These observations are in line with the results reported by Pérez-Masiá et al. (2015) for dextran
424 capsules containing a mixture of soybean oil and lycopene, and by Gómez-Mascaraque and López-
425 Rubio (2016) for gelatin, SPI and WPC capsules containing α -linolenic acid. It is also worth noting
426 that dextran capsules containing neat oil had a broader size distribution with larger diameters (>3000
427 nm) than dextran particles with emulsified oil (Fig. 5d). This may be attributed to differences in the
428 droplet size distribution of the dextran solutions containing emulsified (fine emulsion) or neat oil
429 (coarse emulsion). This is in agreement with the findings of Gómez-Mascaraque and López-Rubio
430 (2016) who reported that the emulsification process, which determines the size of the oil droplets, had
431 an important influence on the size of the electrosprayed capsules. These authors observed that capsules
432 with a lower diameter were obtained when employing an intense homogenization process (e.g. Ultra-
433 Turrax followed by ultrasounds), which resulted in smaller oil droplets when compared to the use of a
434 less intense emulsification treatment (e.g. only Ultra-Turrax). Similar morphologies, than the ones
435 previously described, were found for dextran capsules produced at pilot-plant scale (Fig. S5 of the
436 Supplementary Material). Similar to pullulan fibers, both types of capsules obtained in pilot-plant
437 scale (with emulsified and neat oil) presented a reduced size when compared to the ones obtained in
438 lab scale. This was also most likely due to the superior voltage employed in pilot-plant scale which
439 increased the electrostatic repulsive force favoring the disruption of the droplets (Ghorani & Tucker,
440 2015).

441 3.3.2 Lipid encapsulation and distribution

442 To verify that fish oil was not completely degraded during the electrohydrodynamic processing, FTIR
443 analysis was carried out. For that purpose, the characteristic bands of fish oil not overlapping with the
444 infrared bands of the encapsulating biopolymers (e.g. pullulan and dextran) were identified. Fig. 6
445 shows ATR-FTIR spectra of fish oil, control NMS without fish oil (e.g. only biopolymer and Tween
446 20), and NMS with emulsified or neat oil. It was found that many of the characteristic bands of fish oil
447 overlapped with infrared bands of pullulan, dextran or both; which did not allow to identify potential
448 interactions between the polymers and the oil. Nevertheless, the following differences (marked by
449 arrows in Fig. 6a-b) between the control NMS and NMS containing fish oil were observed: i)
450 characteristic bands for functional groups of alkanes, attributed to C-H stretching vibrations, with
451 wavenumbers $3000 - 2700 \text{ cm}^{-1}$, particularly a band at 2854 cm^{-1} corresponding with -C-H (CH_2 and
452 CH_3 groups, symmetrical stretching); and ii) a band at 1746 cm^{-1} corresponding to the -C=O group of
453 triglycerides (ester stretching) (Guillén & Cabo, 1998; Hamilton & Cast, 1999). Thus, the presence of
454 fish oil in the NMS was confirmed by the appearance of these two characteristic bands of fish oil.
455 Likewise, these infrared bands were selected by Pérez-Masiá et al. (2015) to confirm the presence of
456 soybean and lycopene in dextran capsules. It should be mentioned that the intensity of these bands
457 were similar for both pullulan fibers with emulsified and neat oil (Fig. 6a), but differences were
458 observed between the dextran capsules (Fig. 6b). Dextran capsules with neat oil showed a lower
459 intensity for the two bands, indicating that less oil was incorporated or that the oil was degraded
460 during the process. The decreased oil content could be due to an observed phase separation for the
461 dextran solution containing neat oil during the electro spraying process, further commented below.

462 The methodology selected to incorporate the fish oil to the polymer solution had a statistically
463 significant influence on the EE values obtained. For both types of biopolymers (pullulan and dextran),
464 incorporating the oil as emulsified oil led to lower values of EE (69.1 ± 0.2 and 68.3 ± 0.3 %,
465 respectively) when compared to the EE obtained when adding neat oil (89.6 ± 0.7 and 75.5 ± 0.9 ,
466 respectively). It is of great importance to obtain high EE values when working with omega-3 PUFA,
467 since the encapsulation affects the exposure of the bioactive compound to prooxidants (e.g. oxygen,

468 light, free radicals, metal ions), both during storage of the NMS and when incorporated into food
469 systems. Apart from the EE value of pullulan fibers containing neat oil, the EE values obtained in this
470 study are considerably lower than those reported by Moomand and Lim (2014) for zein fibers loaded
471 with fish oil (91.2 ± 1.1 %). The presence of surface oil was also supported by the wet-STEM in E-
472 SEM image shown in Fig. 7a. For pullulan fibers, both encapsulated and non-entrapped oil droplets
473 could be differentiated (blue and red arrows in Fig. 7a, respectively). Small particles sitting on the
474 fibers, which could indicate the presence of surface oil, were also observed in the cryo-SEM images of
475 the fibers (marked by white arrows in Fig. 4b-c). These small features in the surface of the fibers were
476 more abundant in fibers containing emulsified than neat oil; which correlated well with the EE values.
477 This might be related to the fact that in fibers with neat oil the lipids were mostly located in beads,
478 which minimized the specific surface area and thereby reducing the interactions with the solvent used
479 to extract the surface oil in the analysis. For dextran particles, Fig. 7b shows a capsule with a dense
480 core and small darker circles (marked with blue arrows) which are attributed to the presence of either
481 small dextran particles or oil droplets sitting inside the capsules. These areas with higher contrast
482 appear blurred in all our micrographs indicating that these small dextran particles or oil droplets are
483 placed in the interior of the dextran capsule. Staining the NMS with OsO_4 was not selective for the
484 lipids, and therefore did not help locating the presence of encapsulated or surface oil in neither dextran
485 particles nor pullulan fibers (see Fig. S6 of the Supplementary Material).

486 **3.3.3 Oxidative stability**

487 Table 2 shows the content of hydroperoxides and selected secondary oxidation products (e.g. 1-
488 penten-3-ol, hexanal and nonanal) of pullulan fibers and dextran particles right after their production.
489 For pullulan fibers, the methodology used to add the oil to the electrospinning solution (emulsified or
490 neat) had a great influence on the oxidative status of the fibers. In lab scale, it was found that fibers
491 containing neat fish oil presented a significantly lower PV than fibers with emulsified oil when
492 running batches of 120 and 30 min. The same trend was found for the content of the fibers in 1-
493 penten-3-ol, a volatile product derived from the oxidation of omega-3 fatty acids. This correlated well
494 with the lower EE values obtained for fibers with emulsified oil, implying more surface oil which is

495 unprotected against prooxidants. These results are in accordance with the higher oxidative stability
496 obtained for zein fibers loaded with fish oil when increasing fish oil entrapment from 91.2 to 95.9 %
497 (Moomand & Lim, 2014). Furthermore, the larger beaded structures present in the fibers with neat oil,
498 where the oil is mainly located, may have led to a greater protection of fish oil against oxidation than
499 in fibers with emulsified oil presenting smaller droplets which increases the specific surface area.
500 Similarly, Moomand and Lim (2014) reported a higher oxidative stability for isopropanol-based zein
501 fibers, having large beads, when compared to beadless ethanol fibers due to its smaller surface-to-
502 volume ratio. Besides, incorporating the oil as neat oil avoided lipid oxidation happening during the
503 homogenization process required to produce the emulsified oil (Serfert, Drusch, & Schwarz, 2009).
504 Additionally, decreasing the duration of the production batch from 120 to 30 min, which reduces the
505 exposure of the surface oil, decreased significantly the PV of fibers both with emulsified and neat oil
506 and the content of 1-penten-3-ol for fibers with emulsified oil (Table 2). Likewise, fiber production at
507 pilot-plant scale, which implied shorter batches (10 min), led to significantly less oxidation of fibers
508 with emulsified oil when compared to production at lab scale; whereas no significant differences were
509 found for fibers with neat oil in terms of PV and volatiles. Therefore, pullulan fibers containing neat
510 oil and produced at lab scale in batches of 30 min exhibited the lowest oxidation after production, with
511 the lowest PV (12.3 ± 0.9 meq O_2 /kg) and the lowest content of 1-penten-3-ol (15.5 ± 5.1 ng/g).
512 Nonetheless, it is worth mentioning that pullulan fibers evaluated in this study had a high content of
513 other volatiles such as hexanal and nonanal, which are derived from oxidation of omega-6 and omega-
514 9 fatty acids, respectively. Although the concentration of these volatiles increased with the duration of
515 the production time, they were also present in the control sample (only containing pullulan and
516 Tween20). This indicated that they were already present in the biopolymer or they were obtained as
517 consequence of degradation of pullulan, as concluded from the volatiles analysis of pullulan fibers not
518 containing Tween20 (unpublished data). In any case, these results denoted a superior oxidative
519 stability of pullulan fibers containing neat oil when compared to other fibers produced using other
520 polymers such as PVA (García-Moreno et al., 2016).

521 Electrospayed dextran capsules containing emulsified oil showed a low oxidative stability (PV>40
522 meq O₂/kg) after production both in lab and pilot-plant scales (Table 2). This might be attributed to the
523 opened-part of the capsules which could allow the leaking of oil from the dextran matrix and it may
524 also be attributed to the presence of surface oil. Even though the duration of the batch production was
525 reduced from 120 to 10 min, production in pilot-plant scale led to a higher content of PV and volatiles
526 when compared to lab scale. This is explained by the presence of droplets in the collector, as a
527 consequence of the lack of optimization of the solution for working in the vertical configuration of the
528 pilot-plant equipment. Contrary to pullulan fibers, the addition of neat fish oil instead of emulsified
529 did not enhance lipid protection. Although the volatiles content was reduced when working in lab
530 scale with a horizontal configuration, a high PV (>40 meq O₂/kg) with a large standard deviation was
531 still obtained. This may be due to the fact that the solution was not stable during the electrospaying
532 process, experiencing phase separation which led to capsules with not homogenous composition (lipid
533 content of 7.7±3.4 wt.% instead of the theoretical 12.0 wt.%). In pilot-plant scale, a significantly lower
534 PV (21.2±9.5 meq O₂/kg) was obtained for capsules with neat oil when compared to capsules with
535 emulsified oil. However, the phase separation of the dextran solution contained neat oil was even more
536 severe in pilot-plant scale, probably due to the long tube connecting the syringe and the needles and to
537 the vertical configuration, leading to capsules with a lipid content of 2.1±0.2 wt.%. These results
538 indicated that future studies are required in order to: i) produce physically stable dextran solutions
539 containing neat fish oil (e.g. using Ultraturrax and/or high pressure homogenizers), and ii) optimize
540 solutions composition and electrospaying processing variables (flowrate, voltage and distance) which
541 allow to only obtain fine particles in the collector (e.g. no droplets). Similarly to our results, Gómez-
542 Mascaraque and López-Rubio (2016) reported a low protection of α-linolenic acid when encapsulated
543 in gelatin capsules by electrospaying, even when capsules with an appropriate morphology were
544 obtained.

545 **4. CONCLUSIONS**

546 Carbohydrate-based NMS containing fish oil were successfully obtained by using pullulan and
547 dextran. Pullulan (15 wt.%) and dextran 70 kDa (25 wt.%) solutions presented adequate properties to
548 allow the formation by electrohydrodynamic processing of nano-microfibers and nano-microcapsules,
549 respectively. Dextran particles showed a low oxidative stability both when adding the oil as emulsified
550 or neat oil in lab and pilot-plant scale. The low oxidative stability may be attributed to a poor
551 interaction between the polymer and the fish oil which led to phase separation of the electrospinning
552 solution, capsules with an opened-part and oil on the surface. On the other hand, pullulan fibers with
553 neat oil produced in small batches (30 or 10 min at lab or pilot-plant scale, respectively) exhibited a
554 superior oxidative stability after production, compared to fibers containing emulsified oil. The
555 superior oxidative stability of fibers with neat oil was most likely due to a high EE (89.6 ± 0.7), due to
556 the location of fish oil in bead-structures which implied a lower specific surface area, and due to the
557 elimination of the homogenization process. These promising results may open-up new opportunities for
558 the utilization of pullulan as biopolymer for encapsulation of omega-3 PUFA and other heat-sensitive
559 bioactives by electrospinning.

560 **ACKNOWLEDGEMENTS**

561 This work was supported by the European Commission (ELECTRONANOMEGA project). P.J.
562 García-Moreno acknowledges a Marie-Curie postdoctoral fellowship (Grant Agreement 654818). J.M.
563 Lagaron would like to thank the Spanish Ministry of Economy and Competitiveness (MINECO)
564 project AGL2015-63855-C2-1-R for financial support. The authors are also grateful to Dr. Celia
565 Libran from Bioinicia S.L. for experimental support with the electrospinning equipment in pilot-plant
566 scale.

567 **REFERENCES**

568 Aceituno-Medina, M., Mendoza, S., Lagaron, J. M., & López-Rubio, A. (2015). Photoprotection of
569 folic acid upon encapsulation in food-grade amaranth (*amaranthus hypochondriacus* L.) protein isolate
570 - pullulan electrospun fibers. *LWT - Food Science and Technology*, 62, 970-975.

- 571 Alborzi, S., Lim, L. -, & Kakuda, Y. (2010). Electrospinning of sodium alginate-pectin ultrafine
572 fibers. *Journal of Food Science*, 75, C100-C107).
- 573 AOCS (1998a). AOCS Official Method Ce 2e66. Preparation of Methyl Esters of Long Chain Fatty
574 Champaign: AOCS Press.
- 575 AOCS (1998b). AOCS Official Method Ce 1be89. Fatty Acid Composition by GLC, Marine Oils.
576 Champaign: AOCS Press.
- 577 AOCS (1998c). AOCS Official method Ce 8-89. Determination of tocopherols and tocotrienols in
578 vegetable oils and fats by HPLC. Champaign: AOCS Press.
- 579 Arecchi, A., Mannino, S., & Weiss, J. (2010). Electrospinning of Poly(vinyl alcohol) Nanofibers
580 Loaded with Hexadecane Nanodroplets. *Journal of Food Science*, 75, N80–N88.
- 581 Bakry, A. M., Fang, Z., Ni, Y., Cheng, H., Chen, Y. Q., & Liang, L. (2016). Stability of tuna oil and
582 tuna oil/peppermint oil blend microencapsulated using whey protein isolate in combination with
583 carboxymethyl cellulose or pullulan. *Food Hydrocolloids*, 60, 559-571.
- 584 Barrow, C.J., Wang, B., Adhikari, B., & Liu, H. (2013). Spray drying and encapsulation of omega-3
585 oils. In: C. Jacobsen, N. S. Nielsen, A. F. Horn, & A.D.M. Sørensen (Eds.), *Food Enrichment with*
586 *Omega-3 Fatty Acids* (pp. 194-225). Cambridge: Woodhead Publishing Ltd.
- 587 Bhardwaj, N., & Kundu, S. C. (2010). Electrospinning: A fascinating fiber fabrication technique.
588 *Biotechnology Advances*, 28, 325-347.
- 589 Bligh, E. G., & Dyer, W. J. (1959). A rapid method for total lipid extraction and purification.
590 *Canadian Journal of Biochemistry and Physiology*, 37, 911–917.
- 591 Brahatheeswaran, D., Mathew, A., Aswathy, R. G., Nagaoka, Y., Venugopal, K., Yoshida, Y., et al.
592 (2012). Hybrid fluorescent curcumin loaded zein electrospun nanofibrous scaffold for biomedical
593 applications. *Biomedical Materials*, 7, 045001.
- 594 Chanamai, R., & McClements, D. J. (2001). Depletion flocculation of beverage emulsions by gum
595 arabic and modified starch. *Journal of Food Science*, 66, 457-463.

- 596 Cho, D., Netravali, A. N., & Joo, Y. L. (2012). Mechanical properties and biodegradability of
597 electrospun soy protein Isolate/PVA hybrid nanofibers. *Polymer Degradation and Stability*, 97, 747-
598 754.
- 599 Chronakis, I. S. (2010). Nano-microfibers by Electrospinning Technology: Processing, Properties and
600 Applications. In Y. Quin (Ed.), *Micromanufacturing Engineering and Technology* (pp. 264-286).
601 Oxford: Elsevier.
- 602 Comunian, T. A., & Favaro-Trindade, C. S. (2016). Microencapsulation using biopolymers as an
603 alternative to produce food enhanced with phytosterols and omega-3 fatty acids: A review. *Food*
604 *Hydrocolloids*, 61, 442-457.
- 605 Encina, C., Vergara, C., Giménez, B., Oyarzún-Ampuero, F., & Robert, P. (2016). Conventional
606 spray-drying and future trends for the microencapsulation of fish oil. *Trends in Food Science &*
607 *Technology*, 56, 46-60.
- 608 Fathi, M., Martín, T., & McClements, D. J. (2014). Nanoencapsulation of food ingredients using
609 carbohydrate based delivery systems. *Trends in Food Science and Technology*, 39, 18-39.
- 610 García-Moreno, P.J., Stephansen, K., Van Der Kruijs, J., Guadix, A., Guadix, E. M., Chronakis, I. S.,
611 & Jacobsen, C. (2016). Encapsulation of fish oil in nanofibers by emulsion electrospinning: Physical
612 characterization and oxidative stability. *Journal of Food Engineering*, 183, 39-49.
- 613 García-Moreno, P. J., Guadix, A., Guadix, E. M., & Jacobsen, C. (2016). Physical and oxidative
614 stability of fish oil-in-water emulsions stabilized with fish protein hydrolysates. *Food Chemistry*, 203,
615 124-135.
- 616 Ghorani, B., & Tucker, N. (2015). Fundamentals of electrospinning as a novel delivery vehicle for
617 bioactive compounds in food nanotechnology. *Food Hydrocolloids*, 51, 227-240.
- 618 GOED (2015). GOED Publishes Finished Product Report. URL
619 ([http://goedomega3.com/index.php/the-goed-current-editorials/goed-publishes-finished-product-](http://goedomega3.com/index.php/the-goed-current-editorials/goed-publishes-finished-product-report)
620 [report](http://goedomega3.com/index.php/the-goed-current-editorials/goed-publishes-finished-product-report)) (accessed October 2016).

- 621 Gómez-Mascaraque, L. G., Sanchez, G., & López-Rubio, A. (2016a). Impact of molecular weight on
622 the formation of electrosprayed chitosan microcapsules as delivery vehicles for bioactive compounds.
623 *Carbohydrate Polymers*, 150, 121-130.
- 624 Gomez-Mascaraque, L. G., Morfin, R. C., Pérez-Masiá, R., Sanchez, G., & Lopez-Rubio, A. (2016b).
625 Optimization of electrospraying conditions for the microencapsulation of probiotics and evaluation of
626 their resistance during storage and in-vitro digestion. *LWT - Food Science and Technology*, 69, 438-
627 446.
- 628 Gómez-Mascaraque, L. G., & López-Rubio, A. (2016). Protein-based emulsion electrosprayed micro-
629 and submicroparticles for the encapsulation and stabilization of thermosensitive hydrophobic
630 bioactives. *Journal of Colloid and Interface Science*, 465, 259-270.
- 631 Guillén, M.D., & Cabo, N. (1998). Relationships between the Composition of Edible Oils and Lard
632 and the Ratio of the Absorbance of Specific Bands of Their Fourier Transform Infrared Spectra. Role
633 of Some Bands of the Fingerprint Region. *Journal of Agriculture and Food Chemistry*, 46, 1788-1793.
- 634 Hamilton, R.J., & Cast, J. (1999). Spectral properties of lipids. Boca Raton, CRC press.
- 635 Lertsutthiwong, P., & Rojsitthisak, P. (2011). Chitosan-alginate nanocapsules for encapsulation of
636 turmeric oil. *Pharmazie*, 66, 911-915.
- 637 Li, J., He, A., Zheng, J., & Han, C. C. (2006). Gelatin and gelatin - hyaluronic acid nanofibrous
638 membranes produced by electrospinning of their aqueous solutions. *Biomacromolecules*, 7, 2243-
639 2247.
- 640 Lim, L.T. (2015). Encapsulation of bioactive compounds using electrospinning and electrospraying
641 technologies. In C.M. Sabliov, H. Chen, R.Y. Yada (Eds.), *Nanotechnology and Functional Foods:
642 Effective Delivery of Bioactive Ingredients* (pp. 297-317). New York: John Wiley & Sons.
- 643 Lopes Da Silva, J. A. (2012). Functional nanofibers in food processing. In Q. Wei (Ed.), *Functional
644 nanofibers and their applications* (pp. 262-304). Cambridge: Woodhead Publishing.

- 645 López-Rubio, A., Sanchez, E., Wilkanowicz, S., Sanz, Y., & Lagaron, J. M. (2012). Electrospinning
646 as a useful technique for the encapsulation of living bifidobacteria in food hydrocolloids. *Food*
647 *Hydrocolloids*, 28, 159-167.
- 648 López-Rubio, A., & Lagaron, J. M. (2012). Whey protein capsules obtained through electrospaying
649 for the encapsulation of bioactives. *Innovative Food Science and Emerging Technologies*, 13, 200-
650 206.
- 651 Matsumura, Y., Egami, M., Satake, C., Maeda, Y., Takahashi, T., Nakamura, A., & Mori, T. (2003).
652 Inhibitory effects of peptide-bound polysaccharides on lipid oxidation in emulsions. *Food Chemistry*,
653 83, 107-119.
- 654 Moomand, K., & Lim, L. -. (2014). Oxidative stability of encapsulated fish oil in electrospun zein
655 fibres. *Food Research International*, 62, 523-532.
- 656 Moomand, K., & Lim, L.-T. (2015). Effects of solvent and n-3 rich fish oil on physicochemical
657 properties of electrospun zein fibres. *Food Hydrocolloids*, 46, 191-200.
- 658 Neo, Y. P., Ray, S., Jin, J., Gizdavic-Nikolaidis, M., Nieuwoudt, M. K., Liu, D., et al. (2013).
659 Encapsulation of food grade antioxidant in natural biopolymer by electrospinning technique: a
660 physicochemical study based on zeinegallic acid system. *Food Chemistry*, 136, 1013-1021.
- 661 Park, J.K., & Khan, T. (2009). Other microbial polysaccharides: pullulan, scleroglucan, elsinan, levan,
662 alternant, dextran. In: Phillips, G.O. and Williams, P.A. (Eds.), *Handbook of Hydrocolloids* (pp. 592-
663 614). Cambridge: Woodhead Publishing Ltd.
- 664 Pérez-Masiá, R., Lagaron, J. M., & López-Rubio, A. (2014). Development and optimization of novel
665 encapsulation structures of interest in functional foods through electrospaying. *Food and Bioprocess*
666 *Technology*, 7, 3236-3245.
- 667 Pérez-Masiá, R., Lagaron, J. M., & Lopez-Rubio, A. (2014). Surfactant-aided electrospaying of low
668 molecular weight carbohydrate polymers from aqueous solutions. *Carbohydrate Polymers*, 101, 249-
669 255.

- 670 Pérez-Masiá, R., Lagaron, J. M., & López-Rubio, A. (2015). Morphology and stability of edible
671 lycopene-containing micro- and nanocapsules produced through electrospraying and spray drying.
672 *Food and Bioprocess Technology*, 8, 459-470.
- 673 Ramakrishna, S. (2005). *An Introduction to Electrospinning and Nanofibers*. Singapore: World
674 Scientific.
- 675 Ritcharoen, W., Thaiying, Y., Saejeng, Y., Jangchud, I., Rangkupan, R., Meechaisue, C., & Supaphol,
676 P. (2008). Electrospun dextran fibrous membranes. *Cellulose*, 15, 435-444.
- 677 Serfert, Y., Drusch, S., & Schwarz, K. (2009). Chemical stabilisation of oils rich in long-chain
678 polyunsaturated fatty acids during homogenisation, microencapsulation and storage. *Food Chemistry*,
679 113, 1106–1112
- 680 Singh, H., & Ye, A. (2009). Interactions and Functionality of Milk Proteins in Food Emulsions. In A.
681 Thompson, M. Boland, H. Singh (Eds.), *Milk Proteins: From Expression To Food* (pp. 321-345).
682 London: Elsevier Academic Press Inc.
- 683 Shahidi, F. (2015). Omega-3 fatty acids and marine oils in cardiovascular and general health: A
684 critical overview of controversies and realities. *Journal of Functional Foods*, 19, 797-800.
- 685 Shantha, N. C., & Decker, E. A. (1994). Rapid, sensitive, iron-based spectrophotometric methods for
686 determination of peroxide values of food lipids. *Journal of AOAC International*, 77, 421–424.
- 687 Stijnman, A. C., Bodnar, I., & Hans Tromp, R. (2011). Electrospinning of food-grade polysaccharides.
688 *Food Hydrocolloids*, 25, 1393-1398.
- 689 Tong, L. M., Sasaki, S., McClements, D. J., & Decker, E. A. (2000). Mechanisms of the antioxidant
690 activity of a high molecular weight fraction of whey. *Journal of Agricultural and Food Chemistry*, 48,
691 1473-1478.
- 692 Torres-Giner, S., Martinez-Abad, A., Ocio, M. J., & Lagaron, J. M. (2010). Stabilization of a
693 nutraceutical omega-3 fatty acid by encapsulation in ultrathin electrosprayed zein prolamine. *Journal*
694 *of Food Science*, 75, N69-N79.

- 695 Weiss, J., Kanjanapongkul, K., Wongsasulak, S., & Yoovidhya, T. (2012). Electrospun fibers:
696 Fabrication, functionalities and potential food industry applications. In Q. Huang (Ed.),
697 *Nanotechnology in the food, beverage and nutraceutical industries* (pp. 362-397). Cambridge:
698 Woodhead Publishing Ltd.
- 699 Wongsasulak, S., Patapeejumruswong, M., Weiss, J., Supaphol, P., & Yoovidhya, T. (2010).
700 Electrospinning of food-grade nanofibers from cellulose acetate and egg albumen blends. *Journal of*
701 *Food Engineering*, 98, 370-376.
- 702 Yang, J.-M., Zha, L.-s., Yu, D.-G., & Liu, J. (2013). Coaxial electrospinning with acetic acid for
703 preparing ferulic acid/zein composite fibers with improved drug release profiles. *Colloids and*
704 *Surfaces B: Biointerfaces*, 102, 737e743.

FIGURE AND TABLE CAPTIONS

- Figure 1. SEM images of 5 wt.% pullulan (A), 10 wt.% pullulan (B), 15 wt.% pullulan (C), 20 wt.% dextran70 (D), 30 wt.% dextran70 (E), 40 wt.% dextran70 (F), 10 wt.% dextran500 (G), 20 wt.% dextran500 (H), 30 wt.% dextran500 (I), 10 wt.% WPC (J), 20 wt.% WPC (K), and 30 wt.% WPC (L).
- Figure 2. Peroxide value during storage of biopolymers solutions (15 wt.% pullulan, 30 wt.% dextran70, 20 wt.% dextran500, 30 wt.% WPC) containing fish oil. Emulsion was evaluated as a control.
- Figure 3. Volatiles content during storage of biopolymers solutions (15 wt.% pullulan, 30 wt.% dextran70, 20 wt.% dextran500, 30 wt.% WPC) containing fish oil. Emulsion was evaluated as a control.
- Figure 4. Morphology and diameter distribution of pullulan fibers produced at lab scale: a) control, b) emulsified, c) neat, d) fiber average diameter distribution, e) standard deviation from average diameter, and f) bead diameter distribution.
- Figure 5. Morphology of dextran capsules produced at lab scale: a) control, b) emulsified, and c) neat, and d) diameter distribution.
- Figure 6. AFTR-FITR spectra of NMS produced at pilot-plant scale: a) pullulan fibers, and b) dextran capsules.
- Figure 7. Wet-STEM in E-SEM image of NMS containing neat oil: a) pullulan fibers, and b) dextran capsules.
- Table 1. Solution properties of biopolymer solutions containing emulsified fish oil.
- Table 2. Content of primary and secondary oxidation products of selected NMS after production.

Table 1. Solution properties of biopolymer solutions containing emulsified fish oil.

Sample		Viscosity	Surface tension	Conductivity
Polymer	Concentration (wt.%)	(cP)	(mN/m)	(μ S/cm)
	Emulsion	3.9 \pm 0.1 (100 s ⁻¹)*	46.5 \pm 0.1	921.0 \pm 1.4
Pullulan	5	23.6 \pm 0.3 ^a	55.5 \pm 0.1 ^a	30.8 \pm 0.1 ^a
	10	179.0 \pm 0.2 ^b	56.6 \pm 0.2 ^b	39.9 \pm 0.3 ^b
	15	1,040.0 \pm 26.0 ^c	54.1 \pm 0.3 ^c	128.3 \pm 1.7 ^c
Dextran70	20	44.3 \pm 1.9 ^a	40.6 \pm 1.4 ^a	47.0 \pm 0.1 ^a
	30	201.3 \pm 1.4 ^b	23.1 \pm 0.5 ^b	46.0 \pm 0.2 ^b
	40	1,146.8 \pm 13.5 ^c	18.5 \pm 0.8 ^c	34.5 \pm 0.1 ^c
Dextran500	10	29.5 \pm 0.1 ^a	49.2 \pm 0.2 ^a	4,690.0 \pm 0.1 ^a
	20	181.4 \pm 4.3 ^b	48.3 \pm 0.1 ^b	8,210.0 \pm 14.1 ^b
	30	1,096.5 \pm 31.5 ^c	47.6 \pm 0.1 ^c	7,315.0 \pm 21.2 ^c
WPC	10	4.3 \pm 0.2 ^a (100 s ⁻¹)*	44.9 \pm 0.1 ^a	4,385.0 \pm 91.9 ^a
	20	13.5 \pm 0.3 ^b	44.0 \pm 0.1 ^b	6,580.0 \pm 14.1 ^b
	30	66.0 \pm 0.1 ^c	48.5 \pm 0.2 ^c	7,160.0 \pm 0.0 ^c

Different superscript letters within the same column and the same biopolymer indicate significant differences ($p < 0.05$).

*Solutions exhibiting shear thinning behavior.

Table 2. Content of primary and secondary oxidation products of selected NMS after production.

Polymer	Equipment	Oil incorporation	Batch, min	PV, meq O ₂ /kg	Volatiles, ng/g sample		
					1-penten-3-ol	Hexanal	Nonanal
Pullulan	Lab scale	Emulsified	120	69.2±4.2 ^a	131.8±18.1 ^a	150.7±13.1 ^a	1106.8±85.7 ^a
		Emulsified	30	49.4±5.9 ^b	93.5±5.9 ^b	99.1±7.1 ^b	990.1±32.4 ^a
		Neat	120	37.0±3.2 ^c	24.4±11.7 ^{c,d}	140.9±1.8 ^{a,c}	2575.0±482.3 ^b
		Neat	30	12.3±0.9 ^d	15.5±5.1 ^{c,d}	104.4±28.5 ^{b,c}	1574.9±356.1 ^{a,c}
	Pilot-plant scale	Control		-	1.0±1.4 ^c	60.7±13.5 ^d	1278.7±340.3 ^{a,c}
		Emulsified	10	24.8±4.5 ^d	63.2±2.3 ^e	158.1±9.2 ^a	1944.4±152.1 ^{b,c}
		Neat		16.0±2.2 ^{d,e}	33.7±0.4 ^d	87.6±1.1 ^{b,d}	881.5±136.7 ^a
Dextran	Lab scale	Emulsified	120	48.1±4.0 ^{a,b}	85.7±1.5 ^a	104.7±2.9 ^{a,b}	1250.0±35.6 ^a
		Neat*		43.9±19.8 ^{a,b}	5.1±4.8 ^b	51.5±24.5 ^a	429.6±182.8 ^b
	Pilot-plant scale	Control		-	3.9±3.2 ^b	115.1±6.4 ^b	2264.2±190.0 ^c
		Emulsified	10	62.3±4.5 ^b	136.8±8.6 ^c	513.6±12.0 ^c	12281.8±196.5 ^d
		Neat*		21.2±9.5 ^a	113.3±12.0 ^d	634.7±44.3 ^d	9122.9±180.0 ^e

Different superscript letters within the same column and the same biopolymer indicate significant differences ($p < 0.05$).

*Phase separation of solution.

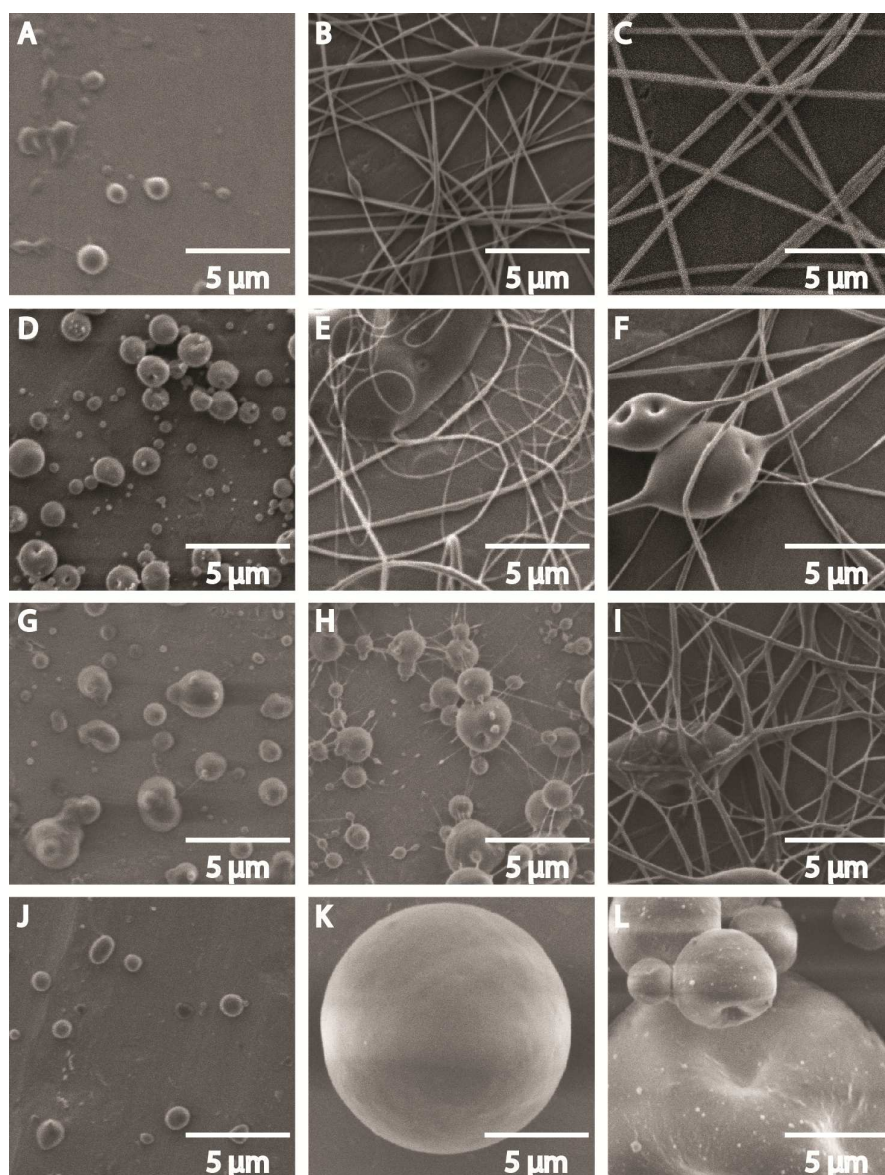


Fig. 1. SEM images of 5 wt.% pullulan (A), 10 wt.% pullulan (B), 15 wt.% pullulan (C), 20 wt.% dextran70 (D), 30 wt.% dextran70 (E), 40 wt.% dextran70 (F), 10 wt.% dextran500 (G), 20 wt.% dextran500 (H), 30 wt.% dextran500 (I), 10 wt.% WPC (J), 20 wt.% WPC (K), and 30 wt.% WPC (L).

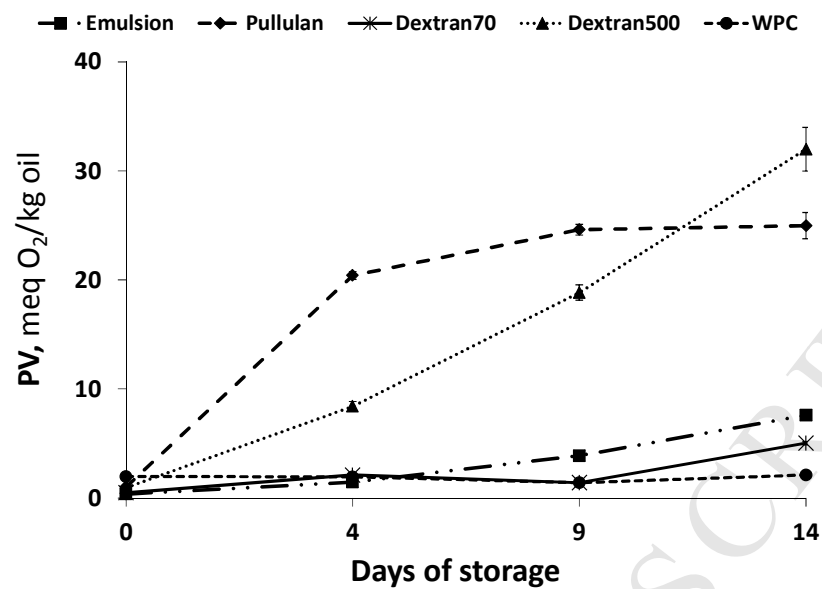


Fig. 2. Peroxide value during storage of biopolymers solutions (15 wt.% pullulan, 30 wt.% dextran70, 20 wt.% dextran500, 30 wt.% WPC) containing fish oil. Emulsion was evaluated as a control.

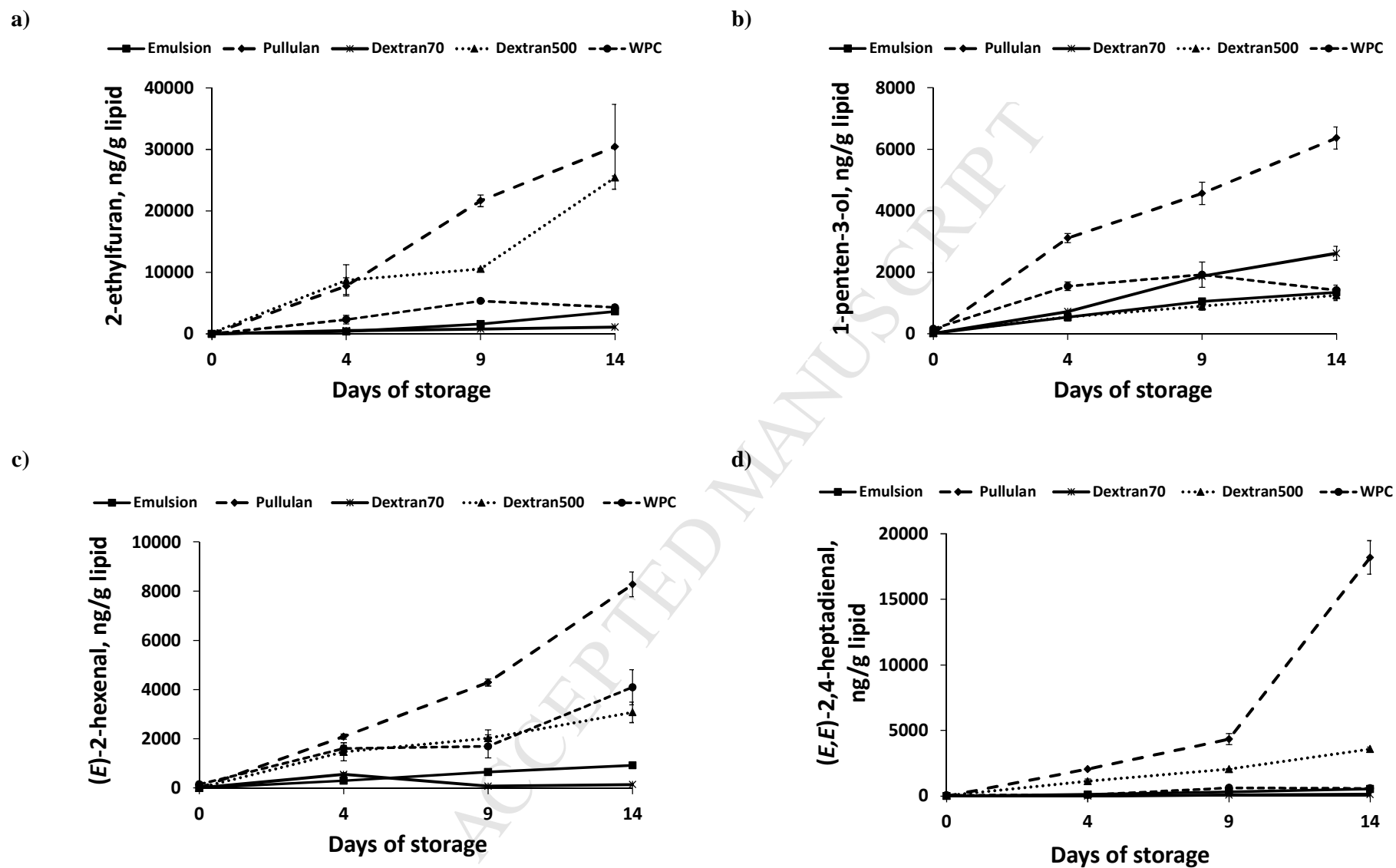


Fig. 3. Volatiles content during storage of biopolymers solutions (15 wt.% pullulan, 30 wt.% dextran70, 20 wt.% dextran500, 30 wt.% WPC) containing fish oil. Emulsion was evaluated as a control.

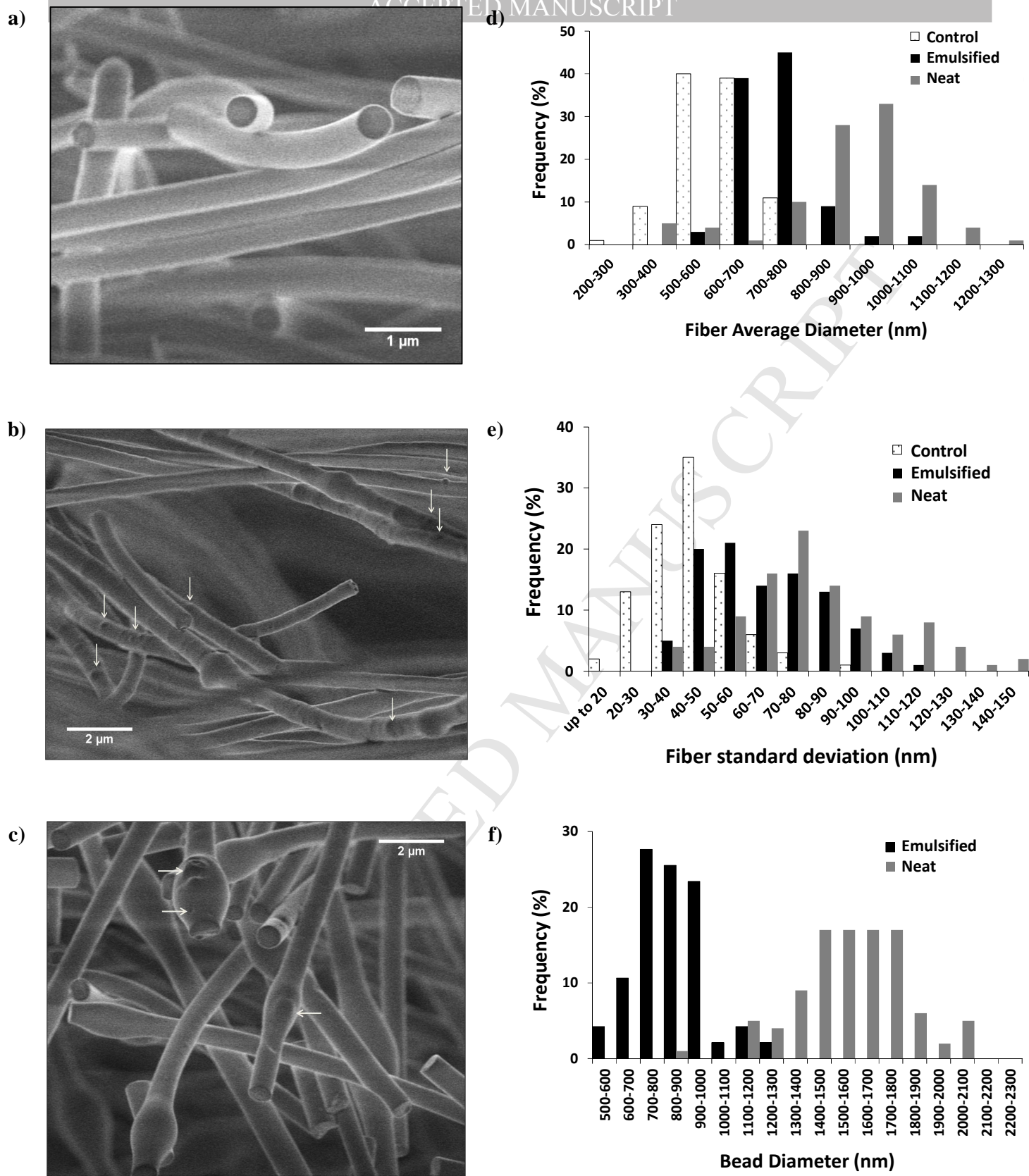


Fig. 4. Morphology and diameter distribution of pullulan fibers produced at lab scale: a) control, b) emulsified, c) neat, d) fiber average diameter distribution, e) standard deviation from average diameter, and f) bead diameter distribution.

The standard deviation from fiber average diameter was calculated by measuring each fiber at 10 different points. A total of one hundred random fibers were measured for this purpose.

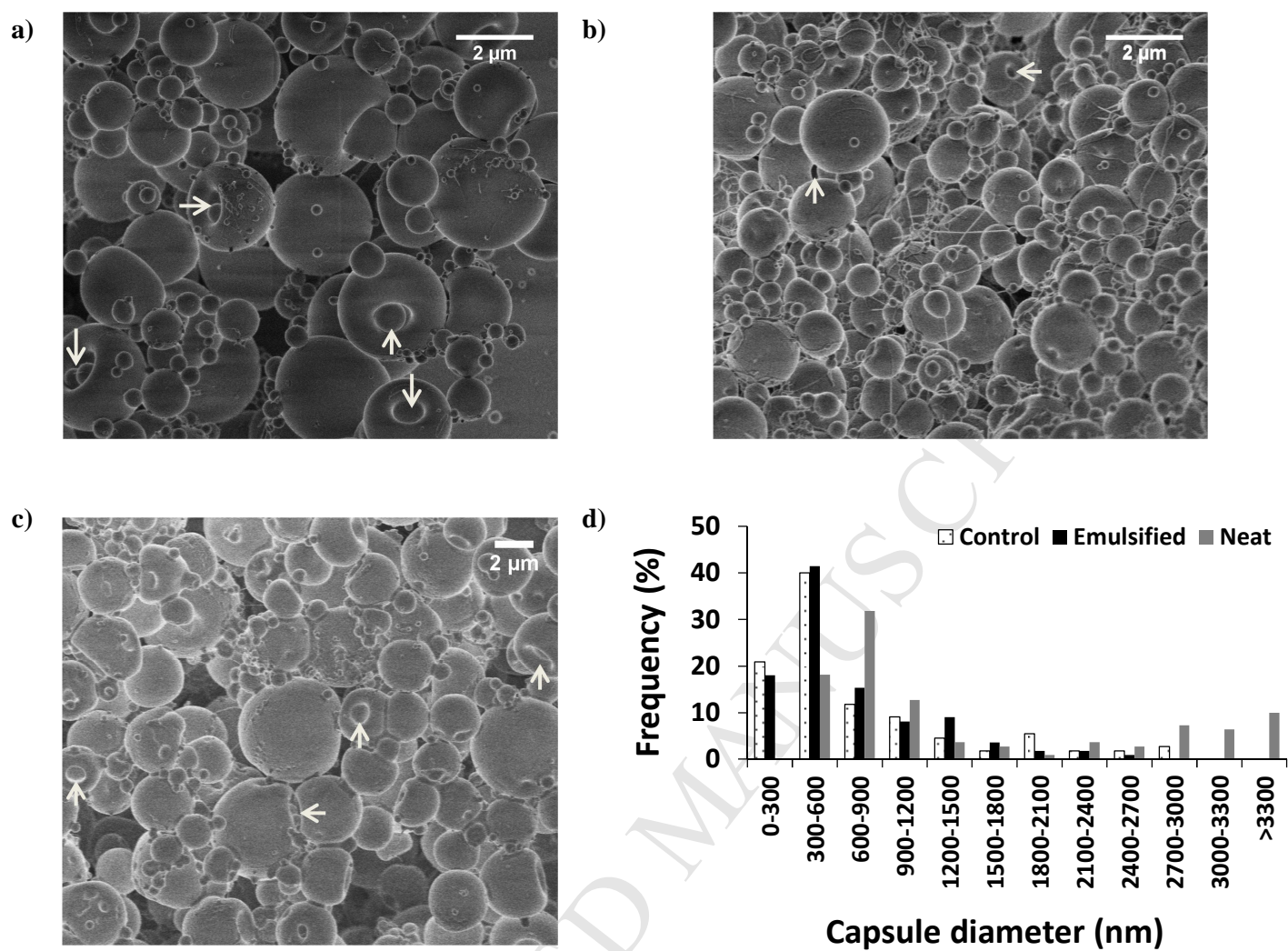


Fig. 5. Morphology of dextran capsules produced at lab scale: a) control, b) emulsified, and c) neat, and d) diameter distribution.

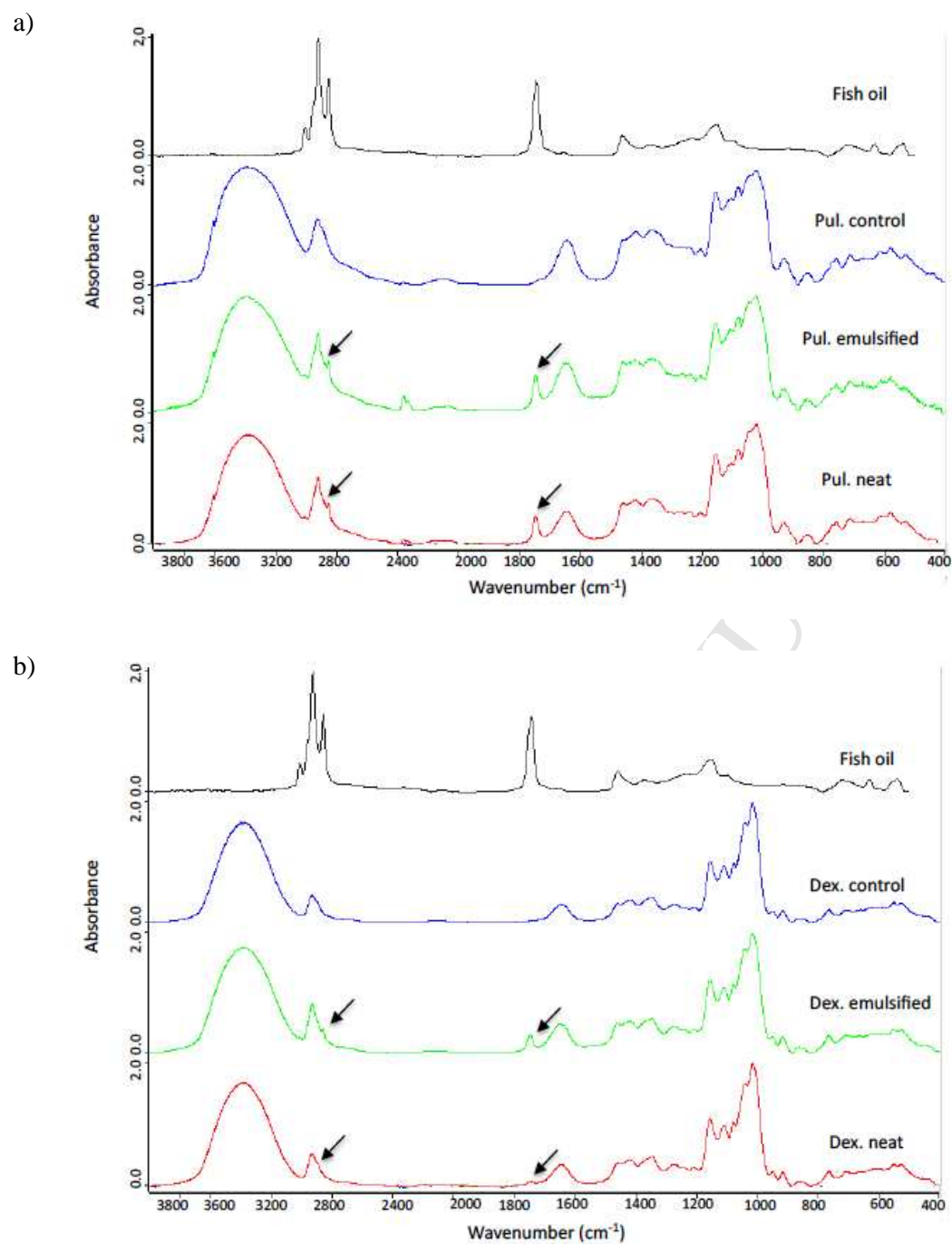


Fig. 6. AFTR-FITR spectra of NMS produced at pilot-plant scale: a) pullulan fibers, and b) dextran capsules.

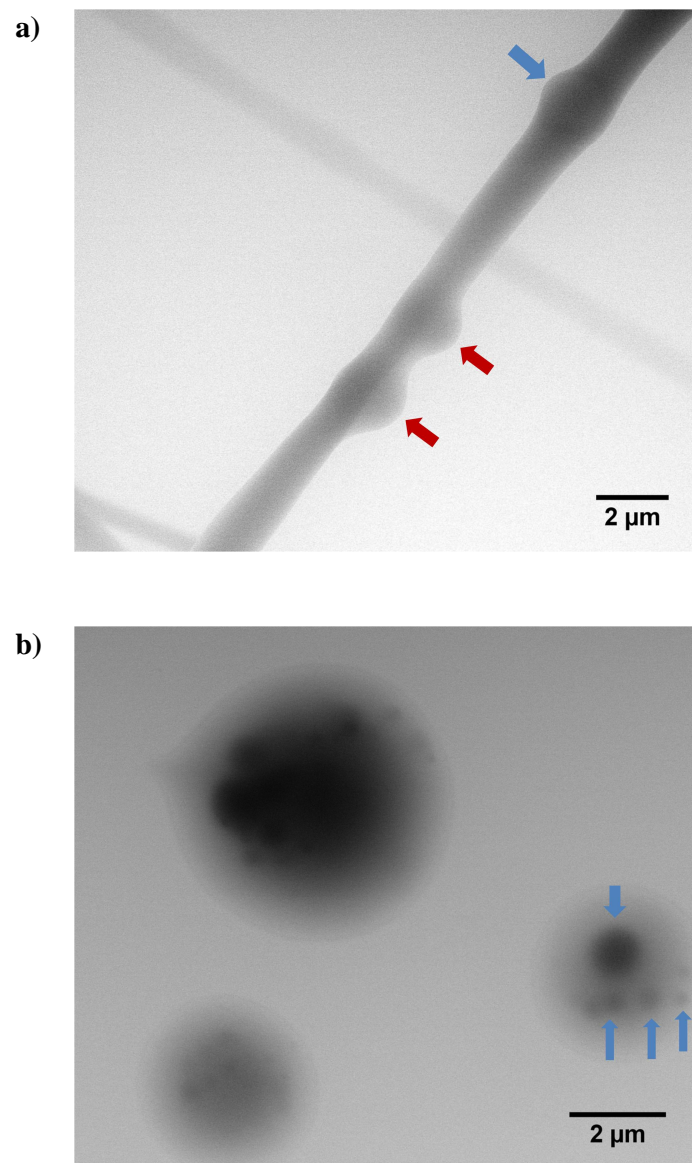


Fig. 7. Wet-STEM in E-SEM image of NMS containing neat oil: a) pullulan fibers, and b) dextran capsules.

Highlights

- Fish oil-loaded nanofibers were produced by electrospinning using pullulan
- Fish oil-loaded capsules were obtained by electrospaying using dextran
- Opened dextran-capsules with poor oxidative stability were obtained
- Oxidatively stable pullulan fibers were produced using neat oil and short batches
- These pullulan nanofibers entrapped the oil efficiently in large bead-structures